Collective and independent-particle motion in doubly excited two-electron atoms

Gregory S. Ezra* and R. Stephen Berry
Department of Chemistry and The James Franck Institute, The University of Chicago, Chicago, Illinois 60637
(Received 22 October 1982)

Configuration-interaction wave functions are calculated for all intrashell doubly excited states of the $N=2$ shell for He and isoelectronic ions Li^+, Be^{2+}, and Ne^{8+} with the use of a basis of Sturmian functions. The density function $\rho(r_1,\theta_{12}\,|\,r_2=\alpha)$, which is the conditional probability that one electron will be found at distance r_1 from the nucleus with interelectronic angle θ_{12} given that the other electron is at distance α from the nucleus, is computed for each of the states and for various values of α. Density plots for the $^1S^e$ states of He are compared with those from Hylleraas-Kinoshita wave functions to assess the quality of the Sturmian basis. Sequences of plots are then examined to investigate the possibility of collective motion in doubly excited states. For He the form of the densities $\rho(r_1,\theta_{12}\,|\,\alpha)$ is in qualitative accord with the molecular model proposed by Kellman and Herrick in that the collective rotational and bending vibrational states are readily identifiable. With increasing nuclear charge a transition occurs to less collective behavior, corresponding to superpositions of hydrogenic configurations associated solely with the $N=2$ shell. Some states, e.g., $^1D^e$, correspond to single independent-particle configurations. Electron density distributions are also presented for the lowest S and P states of the He $n_1=2$, $n_2=3$ intershell manifold with a view to extension of the molecular interpretation to this case. Results are compared with those of calculations of the quantum states of model problems such as particles on concentric spheres.

I. INTRODUCTION

The nature of electron correlation in doubly excited states of two-electron atoms is a problem of considerable theoretical interest (a necessarily incomplete selection of references pertaining to the point of view developed in the present work is given in Refs. 1—22). While the ground state ($1s^2$) and singly excited states ($1snl$) of two-electron atoms can be well represented by a particular zeroth-order configuration, extensive mixing of degenerate and near-degenerate configurations occurs in many doubly excited states so that a description of such states in terms of a dominant single-particle configuration is not possible. In particular, single-particle angular momenta are no longer good quantum numbers. Configuration-interaction (CI) wave functions for doubly excited states have been calculated using very large bases (see, for example, Refs. 23 and 24). However, to gain physical insight into the dynamics of correlation, the central problem is to identify *approximate constants of the motion* to provide new quantum numbers for the classification of doubly excited states.

Work on this problem has proceeded along several different lines. It has been shown by Macek,[5] Fano,[9] and Lin[8] that the two-electron problem exhibits an apparent near separability when expressed in hyperspherical coordinates. Adiabatic channel quantum numbers are approximate constants of the motion in this case, and correspond to particular patterns of radial and angular correlation.[20,21] The fact that the hyperspherical radius is a quasiseparable coordinate is not well understood at present; an analysis of O(6)-symmetry breaking in two-electron systems might clarify the nature of the approximate separability. The detailed effects of nonadiabaticity, i.e., channel mixings, have also yet to be investigated.

Following the pioneering suggestions of Moshinsky,[25] there have been several attempts to treat the problem of correlation in two-electron atoms as a symmetry breaking in the direct-product group $O(4)\times O(4)$.[2,7,10,11,15,16,22] [Recall that the N^2 degenerate states of a hydrogenic system with principal quantum number N span a single irreducible representation of the group O(4), which describes the so-called hidden symmetry of the one-electron atom.][26] Both Wulfman[6] and Herrick and Sinanoglu[7] have shown that for intrashell ($n_1=n_2$) doubly excited states diagonalization of the *difference*

$\vec{B}_1 - \vec{B}_2$ of one-electron Runge-Lenz vectors $\vec{B}_i$ in the manifold of hydrogenic states yields eigenfunctions which are very close to those obtained by diagonalizing the interelectronic repulsion r_{12}^{-1} (for a recent review see Ref. 27). The effectiveness of this operator replacement has been rationalized in classical terms by considering the coupled precession of elliptical single-electron orbits[7,12] (see also Ref. 22).

By defining suitable O(4)-related quantum numbers, Herrick and Kellman were able to organize manifolds of doubly excited states into "supermultiplets" of states,[15,16] and thereby recognize both vibrational and rotational excitations in spectra of two-electron atoms[17] (thus extending earlier work[14] in which rotor series had been recognized). The energy-level patterns were found to correspond to the rotation bending-vibration spectrum of a linear XY_2 triatomic molecule,[28] albeit truncated due to the finite number of states involved. The essential physical picture emerging from this analysis is that, for low values of the nuclear charge at least, doubly excited two-electron systems behave as rather "floppy" XY_2 molecules, exhibiting both collective rotations and bending vibrations. The possibility of such collective motions in atoms is a relatively unfamiliar idea which, as well as providing a simple, physically appealing way of picturing the effects of strong electron correlations, suggests previously unsuspected parallels between atomic and molecular dynamics.[29,30]

The aim of the present work is to investigate whether a naive molecular picture of electron correlation in doubly excited states of two-electron atoms is valid (Fig. 1). That is, to what extent are the two electrons actually localized at roughly the same distance from but on opposite sides of the nucleus, undergoing large-amplitude bending vibrations together with collective rotations? In other words, does a doubly excited atom have a shape? And how does the tendency toward having a shape depend on such factors as nuclear charge?

In order to answer this question, we have undertaken a detailed study of the two-electron density $\rho(r_a, r_2, \theta_{12})$ via the associated conditional probability $\rho(r_1, \theta_{12} \mid r_2 = \alpha)$ for the $N=2$ intrashell doubly excited manifolds of He and isoelectronic ions Li^+, Be^{2+}, and Ne^{8+}. The function $\rho(r_1, \theta_{12}, \mid r_2 = \alpha)$ is the probability of finding an electron at distance r_1 from the nucleus with interelectronic angle θ_{12} given that the other electron is at distance α from the nucleus.[12] It therefore excludes all information concerning the orientation of the electron-nucleus-electron triangle in space, information not directly relevant to the interparticle correlations. Graphs of the conditional probability distribution $\rho(r_1 \theta_{12} \mid r_2 = \alpha)$ have been used previously to study electron correlation in ground [31] and excited S (Refs. 12,13) and P (Ref. 32) states of two-electron atoms represented by CI or Hylleraas-type wave functions, as well as some higher angular momentum doubly excited states described by DESB (doubly excited symmetry basis) -type functions.[12] We present here the first systematic study of a complete doubly excited manifold using high quality CI functions (Sec. II) for all states including P and D angular momentum states.

Previous work[18] using Hylleraas-Kinoshita wave functions for He and H^- showed that the Kellman-Herrick molecular picture is essentially confirmed for S^e and P^o states of the $N=2$ shell, and that the intershell state $2s3s\,^3S^e$ has the character of a first excited antisymmetric vibration. In addition, model studies of the quantum states of electrons on the surface of the same[33] or concentric[34] spheres demonstrated the possibility of pronounced collective motions with characteristic associated rotation-vibration spectra, as well as a smooth transition to independent-particle motions (see also Refs. 35 and 36). In the present work we examine the occurrence of collective motion in real three-dimensional atoms for low values of the nuclear charge and the transition to more familiar independent-particle or single-configuration dynamics as the nuclear charge is increased.

The work presented here is complementary to the recent studies of Lin,[20] who has given extensive graphs of the two-electron density in a series of doubly excited S state channels of He and H^-. Thus, while we plot the density function $\rho(r_1, \theta_{12} \mid r_2 = \alpha)$, Lin prefers to plot the density $\rho(\beta, \theta_{12})$, for fixed values of the hyperradius $R \equiv (r_1^2 + r_2^2)^{1/2}$, where the hyperangle $\beta = \tan^{-1}(r_1/r_2)$. However, whereas the densities we plot are derived from wave functions whose exactness is limited only by the CI procedure itself, the channel functions plotted by Lin are calculated within the adiabatic approximation[9] and so correspond to correlation of two electrons constrained to lie on a hypersphere. Moreover, channels with angular momentum greater than zero have not

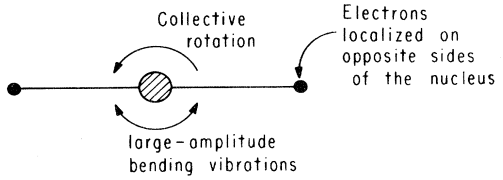

FIG. 1. Molecular picture of electron correlation in doubly excited states of two-electron atoms.

yet been treated graphically by Lin.

The plan of the paper is as follows: Section II and the Appendix are concerned with the details of the choice of basis for our CI calculations on two-electron atoms. Section II outlines our method of computation and provides a detailed comparison between two-electron densities derived from CI and from explicitly correlated Hylleraas-type wave functions for $^1S^e$ states of He in order to assess the quality of basis used, while the Appendix gives details of the Sturmian functions used. In Sec. III we present graphs of densities $\rho(r_1\theta_{12}\,|\,r_2)$ derived from Sturmian CI functions for $N=2$ shell doubly excited states of He, Li^+, Be^{2+}, and Ne^{8+} and discuss the collective or independent-particle-like nature of the states. Section IV gives some results on electron correlation in selected $n_1=2$, $n_2=3$ intershell doubly excited S and P states, with particular attention paid to the extension of the molecular picture to this case. Concluding remarks are given in Sec. V.

II. COMPARISON OF CI AND HYLLERAAS WAVE FUNCTIONS: $^1S^e$ STATES OF He

In this section we consider the choice of basis functions for our two-electron CI calculations. Previous discussions[13,31] of electron correlation in S^e states of He showed graphs of $\rho(r_1,\theta_{12}\,|\,r_2)$ derived from accurate Hylleraas-Kinoshita functions of the form (1):

$$\psi(r_1,r_2,r_{12})=\exp[-\xi(r_1+r_2)]\sum_{\lambda,\mu,\nu} c_{\lambda\mu\nu}(r_1+r_2)^{\lambda}\left[\frac{r_{12}}{r_1+r_2}\right]^{\mu}\left[\frac{r_1-r_2}{r_{12}}\right]^{\nu}. \tag{1}$$

The nonlinear parameter ξ together with the coefficients $c_{\lambda\mu\nu}$ (λ, μ, and ν are integers) were determined using a program written by Roothaan. To study the systematics of electron correlation throughout the entire intrashell doubly excited manifold and, in particular, the phenomenon of collective rotation, we ideally require explicitly correlated wave functions of the form (1) for higher angular momentum states. It is well known, however, that the calculation of such functions presents considerable technical difficulties. (These wave functions have nevertheless been obtained by Bhatia and Temkin[37] and a detailed comparison with our CI functions is in progress.) For this reason, we have chosen in the present work to generate two-electron CI wave functions of the form

$$\psi^j_m(\vec{r}_1,\vec{r}_2)=\sum_{\substack{j_1,\nu_1\\ j_1\nu_2}} c_{j_1\nu_1 j_2\nu_2}\phi_{\nu_1}(r_1)\phi_{\nu_2}(r_2)\times[Y^{j_1}(\hat{r}_1)\times Y^{j_2}(\hat{r}_2)]^j_m \tag{2}$$

and calculate the corresponding densities $\rho(r_1,\theta_{12}\,|\,r_2)$. Here, j and m are the total and azimuthal angular momentum quantum numbers, respectively, and the coupled spherical harmonics are

$$[Y^{j_1}(\hat{r}_1)\times Y^{j_2}(\hat{r}_2)]^j_m \equiv \sum_{m_1,m_2} Y^{j_1}_{m_1}(\hat{r}_1)Y^{j_2}_{m_2}(\hat{r}_2)\langle j_1,m_1,j_2,m_2\,|\,j,m\rangle\,. \tag{3}$$

CI functions of the form (2) are relatively easy to calculate and give a uniform level of approximation for the set of states of interest. As we shall see below, the short-range ($r_{12}\sim 0$) cusp behavior of the accurate wave function is completely absent from the CI functions; however, the questions pertinent to collective, correlated behavior are primarily questions concerning the long-range or global behavior of the electron density, which is generally well represented in our CI functions.

An important question concerns the choice of radial basis functions. It has long been known that,[38] using a complete set of orthonormal hydrogenic one-electron orbitals to expand the two-electron function, it is necessary to include both the discrete spectrum *and* continuum states to ensure convergence to the exact wave function. Since bound-state hydrogenic functions with quantum numbers n and l behave as

$$\phi(r)\sim r^{n-1}e^{-r/n},\quad n>l \tag{4}$$

they rapidly become radially diffuse with increasing principal quantum number n due to the $1/n$ dependence of the exponent. An expansion of intrashell doubly excited state wave functions in a hydrogenic basis might therefore be expected to converge more slowly than an expansion in terms of basis functions whose radial parts are more compact and better localized in the most important regions of configuration space, i.e., $r_1\sim r_2$.

For the CI calculations reported here we have therefore used a Sturmian type of radial basis constructed from Slater orbitals

$$\phi(r)\sim r^{n-1}e^{-\xi r},\quad n>l \tag{5}$$

TABLE I. Calculated energy levels for He doubly excited $N=2$ intrashell states: $-E$ (Ry).

	Sturmian CI[a]	Callaway's Slater CI[b]	Hydrogenic CI[c]	Hylleraas QHQ[d]
$^1S^e$	1.556 06	1.556 79	1.550 49	1.557 63
$^3P^o$	1.520 78	1.519 98	1.516 58	1.522 98
$^3P^e$	1.420 86	1.419 98	1.413 76	1.421 00
$^1D^e$	1.405 99	1.398 70	1.394 96	1.405 63
$^1P^e$	1.385 15	1.381 37	1.376 73	1.385 79
$^1S^e$	1.242 29	1.238 33	1.230 28	1.245 50

[a]The present work.
[b]Reference 24.
[c]Reference 23.
[d]Space of discrete functions (Ref. 37); by using the Feshbach projection-operator technique, the portion of the resonance at $\mathscr{E}$ may be determined variationally by minimizing the functional $\mathscr{E}=\langle\Phi QHQ\Phi\rangle/\langle\Phi Q\Phi\rangle$, where Q is a projection operator such that QHQ has a discrete spectrum.

where the exponent ξ is held *fixed* for fixed values of the single-particle angular momentum l. This basis of radial functions [essentially Laguerre polynomials of order $(2l+1)$] was originally introduced by Hylleraas[39] and has been applied by Holøien[40] and Shull and Löwdin,[41] among others. It is complete with no continuum and is well suited to describe the pronounced angular correlations occurring in intrashell doubly excited states. As we shall see below, in using such a basis it is possible to obtain a good representation of the long-range correlations in the "exact" Hylleraas $^1S^e$ functions. We note also that the elimination of the continuum in favor of a discrete spectrum is characteristic of Lie-algebraic approaches to the one-electron problem.[42]

For *inter*shell doubly excited states, in which the single-particle shell structure leads to localization of the electrons at different distances from the nucleus, a basis of hydrogenic functions may well be more suitable (cf. Sec. IV). Further studies of convergence properties in multiply excited states are needed to determine optimal radial basis sets.

To obtain two-electron densities $\rho(r_1,\theta_{12}\,|\,r_2)$ we therefore proceed as follows:

(a) CI functions of the form (2) are calculated using a radial basis (5) of Sturmian functions. The secular matrix is set up using a modified version of Callaway's program,[24] which evaluates matrix elements of the two-electron Hamiltonian in a symmetrized basis of Slater orbitals. Matrix diagonalization and orthonormalization of the resulting eigenvectors is performed using standard EISPACK routines.[43]

Several comments are in order here. First of all, the doubly excited wave functions we calculate are approximations to the bound-state portions of autoionizing states, which are in fact resonances in the one-electron continuum. Since, in contrast to use of a hydrogenic basis or an explicitly projected Hylleraas basis, use of a nonorthonormal basis of Slater orbitals does not allow lower states ($1s^2$ and $1snl$) to be projected out easily, we must rely on a stabilization method[44] to identify the doubly excited states among the solutions to our secular problem. This means that, except for the $^3P^e$ doubly excited state, which is the lowest of its symmetry type, the energies we find for $N=2$ intrashell states are not necessarily upper bounds to the unshifted resonance energies. Our calculated energies for He are given in Table I, where they are compared with other variational results. It can be seen that agreement with in-

TABLE II. Calculated energy levels for $N=2$ intrashell doubly excited states with Sturmian CI basis: $-E$ (Ry).

	He	Li^+	Be^{2+}	Ne^{8+}
$^1S^e$	1.556 06	3.808 90	7.064 73	47.593 02
$^3P^o$	1.520 78	3.756 21	6.991 10	47.398 32
$^1D^e$	1.405 99	3.545 82	6.681 57	46.473 41
$^1P^o$	1.385 15	3.513 46	6.636 81	46.351 81
$^3P^e$	1.420 86	3.593 06	6.765 13	46.796 73
$^1S^e$	1.242 29	3.257 16	6.270 30	45.341 34

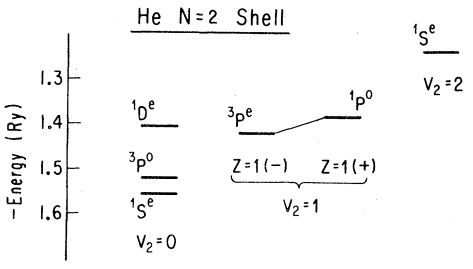

FIG. 2. Calculated energy levels for $N=2$ intrashell doubly excited states of He (Sturmian basis). Assignment of molecular quantum numbers is shown.

dependent calculations is very good. Energies for doubly excited $N=2$ states of He, Li^+, Be^{2+} and Ne^{8+} are shown in Table II. Agreement with the hydrogenic CI values of Lipsky *et al.*[23] is good. Calculated Sturmian CI levels for the six states of the He $N=2$ shell are shown in Fig. 2. We return to the significance of this energy-level pattern below.

In Table IV we list the exponents ξ used to define our orbital basis (5) for nuclear charge $Z=2$, 3, 4, and 10. While we have not performed extensive optimization of the exponents associated with each value of the single-particle angular momentum, it is worth noting that slight screening of the s orbitals greatly improves the stabilization of doubly excited levels. For our calculations we use a single-particle basis with quantum numbers $n \leq 6$ and $l \leq 5$ which gives, for example, a CI basis of maximum dimension 63 for the $^1S^e$ states (see the Appendix).

(b) Having obtained the coefficients $c_{j_1\nu_1 j_2\nu_2}$ in the expansion (2), the next step is to integrate over the Euler angles describing the orientation of the electron-nucleus-electron triangle in space to give $\rho(r_1,r_2,\theta_{12})$, which is the rotational trace of the diagonal two-electron density matrix, expressed in terms of internal variables r_1, r_2, and θ_{12}. This is done using a procedure outlined previously[33] to give

$$\rho(r_1,r_2,\theta_{12}) = \sum_{\substack{j_1,\nu_1,j_2,\nu_2 \\ j_1',\nu_1',j_2',\nu_2'}} c^*_{j_1'\nu_1'j_2'\nu_2'} c_{j_1\nu_1 j_2\nu_2} \phi^*_{\nu_1'}(r_1)\phi^*_{\nu_2'}\phi_{\nu_1}(r_1)\phi_{\nu_2}(r_2)\tfrac{1}{2}[(2j_1'+1)(2j_1+1)(2j_2'+1)(2j_2+1)]^{1/2}$$

$$\times \sum_{k}^{\min(j_1+j_1',j_2+j_2')} (-1)^{j-k}(2k+1) \begin{bmatrix} j_1 & j_1' & k \\ 0 & 0 & 0 \end{bmatrix} \begin{bmatrix} j_2 & j_2' & k \\ 0 & 0 & 0 \end{bmatrix} \begin{Bmatrix} j_1 & k & j_1' \\ j_2' & j & j_2 \end{Bmatrix} P_k(\cos\theta_{12}) \,. \tag{6}$$

(c) Integrating over r_1 and θ_{12} to find the one-particle density $S(r)$,

$$S(r) \equiv \int_0^\infty r_1^2 dr_1 \int_0^\pi \sin\theta_{12} d\theta_{12} \rho(r_1, r_2 = r, \theta_{12}) \,, \tag{7}$$

we finally obtain the conditional probability density $\rho(r_1,\theta_{12} \mid r_2=\alpha)$:

$$\rho(r_1,\theta_{12} \mid r_2=\alpha) \equiv \rho(r_1,r_2=\alpha,\theta_{12})/S(r=\alpha) \,. \tag{8}$$

Integration of (6) over the angle θ_{12} is trivial. Using a radial basis of Slater orbitals the integration over r_1 can be performed analytically. Note that

$$\int_0^\infty r_1^2 dr_1 \int_0^\pi \sin\theta_{12} d\theta_{12} \rho(r_1,\theta_{12} \mid r_2=\alpha) = 1 \,. \tag{9}$$

(d) The conditional probability density $\rho(r_1,\theta_{12} \mid r_2=\alpha)$ [more accurately $r_1^2\rho(r_1,\theta_{12} \mid r_2)$] is then calculated at a grid of r_1,θ_{12} points for given value of r_2 and plotted. In this way we are able to explore the three-dimensional two-electron density as a function of the atom's geometry. The conditional probability density is particularly useful for studying the interaction between "radial" and "angular" correlations of electrons.

Figure 3 shows densities $\rho(r_1\theta_{12} \mid r_2)$ for the "$2s^2$" $^1S^e$ state of He, calculated from the 14-term Hylleraas-Kinoshita function of Ref. 13 and our 63-term Sturmian CI function, respectively, for four values of r_2. The most probable configuration (largest S value) occurs with $r_2 \sim 2.9$ bohr. Comparison of the two sets of graphs shows that the two-electron density associated with our CI function is virtually identical with that for the Hylleraas-Kinoshita function, which explicitly includes terms in the interelectronic distance r_{12}. Note that the most probable configuration ($r_2 \sim 2.9$ bohr) has both electrons at the same distance from but on opposite sides of the nucleus, with a distribution with respect to θ_{12} that is very close to Gaussian. In other words, the lowest $^1S^e$ state of the He $N=2$ manifold is indeed a *rotor state,* qualitatively similar to the rotationless ground state of a linear triatomic molecule XY_2 (Sec. III).[28]

Figure 4 gives a corresponding comparison of Hylleraas-Kinoshita and CI two-electron densities for the upper "$2p^2$" $^1S^e$ state of He. This provides a

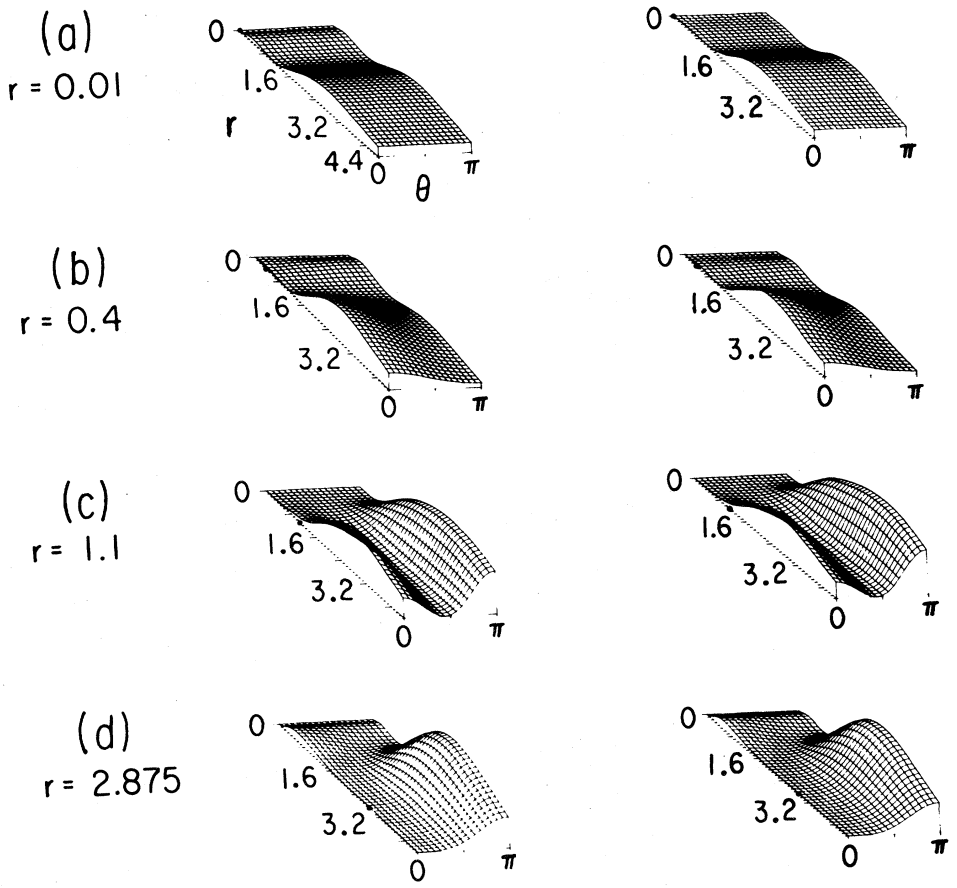

FIG. 3. Comparison of Hylleraas-Kinoshita and Sturmian CI conditional probability densities $\rho(r_1,\theta_{12}\,|\,r_2=\alpha)$ for He "$2s^2$" $^1S^e$ state. (a) $\alpha=0.01$ bohr; (b) $\alpha=0.4$ bohr; (c) $r=1.1$ bohr; (d) $r=2.875$ bohr. The Hylleraas-Kinoshita functions are on the left.

more stringent test of the quality of the Sturmian CI basis we use since the "exact" Hylleraas-Kinoshita function of Ref. 13 shows pronounced angular correlation in this excited state. As can be seen from Fig. 4, our CI function succeeds very well in duplicating the long-range behavior of the two-electron density but fails (as all finite CI expansions in functions not involving r_{12} must) to represent the cusp or "Coulomb hole" around $r_{12}\sim 0$. In the absence of a direct comparison with Hylleraas-type functions for higher angular momentum states, we assume that wave functions of similar accuracy can be obtained for states in the doubly excited manifold with different symmetries. These wave functions are examined in Sec. III. Finally, we note that the He "$2p^2$" $^1S^e$ state is described within the molecular picture as a rotationless state with two quanta of bending vibration. This point is also taken up in Sec. III.

III. $N=2$ INTRASHELL DOUBLY EXCITED STATES: CI FUNCTIONS FOR He, Li^+, Be^{2+}, AND Ne^{8+}

In this section we examine two-electron densities for $N=2$ intrashell doubly excited states of He and isoelectronic ions Li^+, Be^{2+}, and Ne^{8+} calculated using Sturmian CI functions. (In contrast to calculations with a Hylleraas basis, attempts to obtain corresponding eigenvalues and eigenvectors for H^- failed to give stabilized results.) In the following discussion, we point out the occurrence of collective motions for low values of the nuclear charge (He) and discuss the transition to more independent-particle-like dynamics with increasing nuclear charge.

Consider once again Fig. 2, which shows our calculated $N=2$ energy levels for He. The levels have

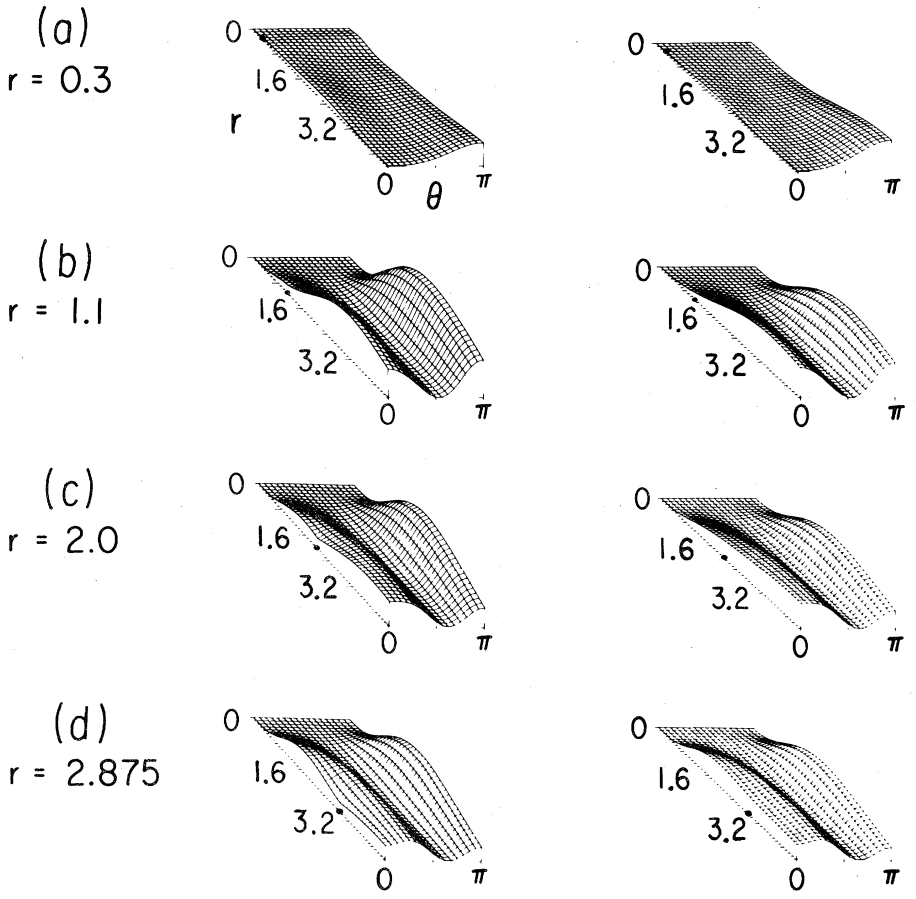

FIG. 4. Comparison of Hylleraas-Kinoshita and Sturmian CI conditional probability densities $\rho(r_1,\theta_{12}\,|\,r_2=\alpha)$ for He "$2p^2$" $^1S^e$ state. (a) $\alpha=0.3$ bohr; (b) $r=1.1$ bohr; (c) $r=2.0$ bohr; (d) $r=2.875$ bohr. The Hylleraas-Kinoshita functions are on the left.

been arranged so as to emphasize the molecular interpretation of the doubly excited spectrum proposed by Kellman and Herrick.[17] Thus, the lowest $^1S^e$ state is interpreted as the ground state of a linear XY_2 triatomic molecule; as seen in Sec. II, the calculated electron density corresponds very closely to this model. In the molecular picture the $^3P^o$ and $^1D^e$ states are members of a rotor series based on the ground $^1S^e$ state, corresponding to overall rotation of the linear electron-nucleus-electron configuration with angular momentum perpendicular to the linear axis. Energies of the He rotor states for $N=2$ fit only very roughly to a $J(J+1)$ rigid-rotor expression, although better fits are obtained for longer sequences of rotor states in higher excited shells. The rotor states $^1S^e$, $^3P^o$, and $^1D^e$ are assigned the bending quantum number $v_2=0$. The near-degenerate $^3P^e$ and $^1P^o$ states then correspond to a pair of levels with one quantum of bending, $v_2=1$, and one unit of vibrational angular momentum along the electron-nucleus-electron axis, $l=1$. By analogy with the case of l doubling in linear polyatomics such as CO_2,[28] the $^3P^e$ and $^1P^o$ states are split by a so-called T doubling.[15,17] Note, however,

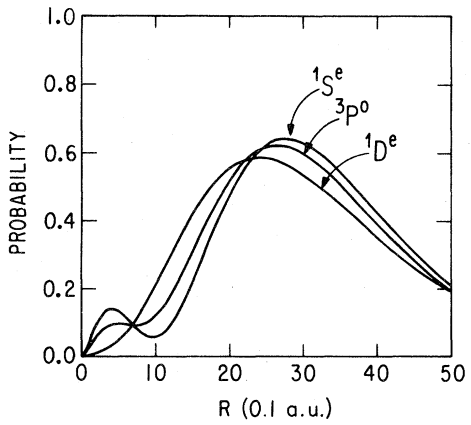

FIG. 5. Single-particle radial distribution function $r^2S(r)$ for He "rotor series": $^1S^e$, $^3P^o$, and $^1D^e$ states.

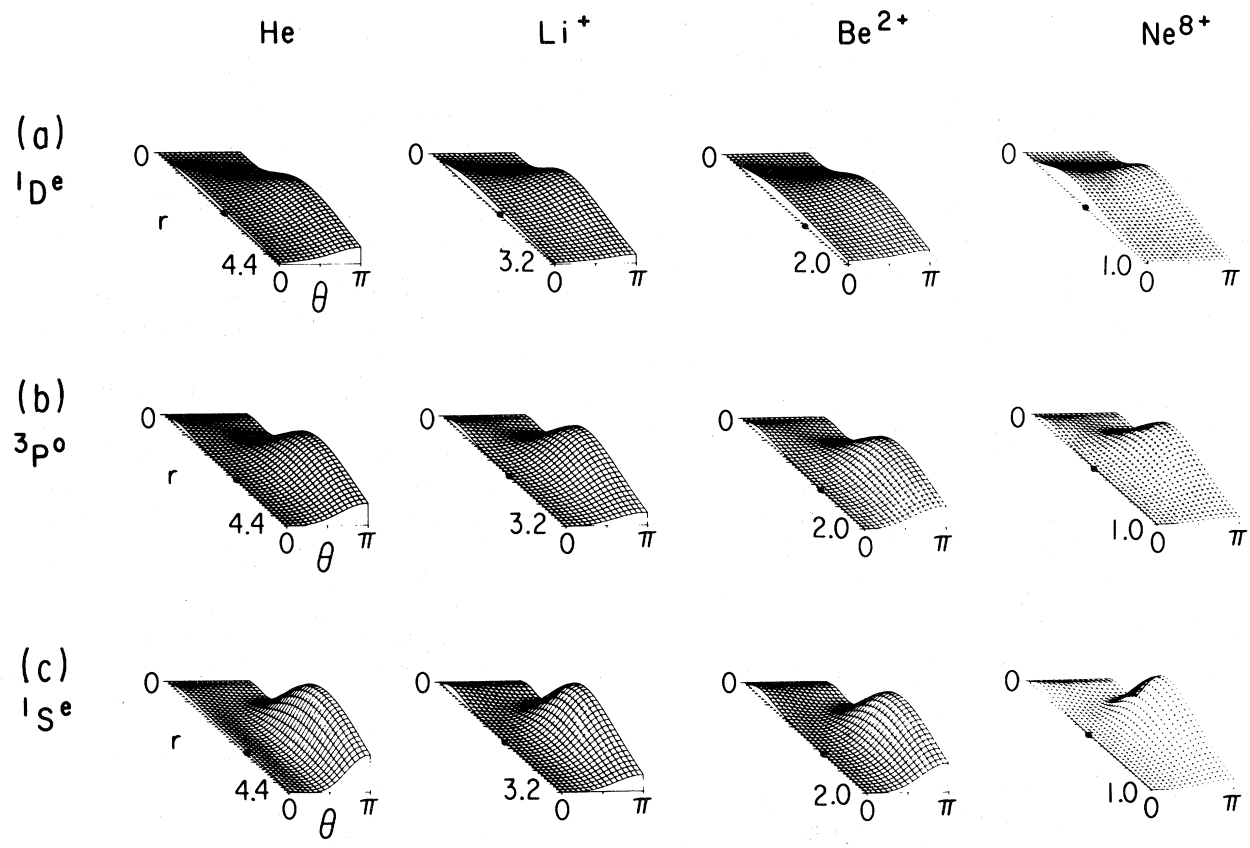

FIG. 6. Conditional probability densities $\rho(r_1,\theta_{12}\,|\,r_2=\alpha)$ for rotor series states $^1S^e$, $^3P^o$, and $^1D^e$. Nuclear charge $Z=2$ (He), 3 (Li^+), 4 (Be^{2+}), and 10 (Ne^{8+}). Radial coordinates have been scaled to facilitate comparison of wave-function shapes; r_2 has its most probable value in each case.

the opposite signs of the splittings in He and linear polyatomics (see below). The molecular interpretation of the He $N=2$ doubly excited manifold is completed by assigning the upper $^1S^e$ level to a rotationless state with two quanta of bending vibration excited, $v_2=2$. We now consider to what extent this molecular model is supported by calculated electron densities.

We first examine the rotor series states. Figure 5 shows the single-particle radial distribution function $r^2S(r)$ for the $^1S^e$, $^3P^o$ and, $^1D^e$ states of He. The plot clearly shows well-defined peaks at the characteristic shell radius 2.5—3.0 bohr. It can also be seen that the one-particle distribution contracts slightly with increasing angular momentum, just as for hydrogenic functions. This result indicates the strong persistence of one-electron radial shell structure in these doubly excited states and is consistent with the finding that a fit of doubly excited levels to molecular term formulas requires a negative centrifugal distortion constant, i.e., the atom "contracts upon rotation."[16,17]

Figure 6 shows conditional probability densities $\rho(r_1,\theta_{12}\,|\,r_2=\alpha)$ for "rotor" states as a function of nuclear charge Z with the value α chosen to correspond to the most probable value in each case, i.e., the peak of the one-particle radial distribution function. The radial coordinates have been scaled for each value of Z to facilitate comparison of the shapes of density distributions. We note that densities for all doubly excited states considered in this work have been studied over extensive ranges of the radial distance r_2; restriction in this paper to most probable values of α is merely to save space while bringing out the essential points as clearly as possible.

Let us compare the $^1S^e$ and $^3P^o$ states of He. The $^3P^o$ density is remarkably similar to that of the $^1S^e$ state at the most probable value of r_2, exhibiting the same angular correlation and localization of the two electrons at the same distance from the nucleus. We therefore conclude that the $^3P^o$ state corresponds to *collective rotation* of the two-electron atom in that there is an intrinsic function or shape which is very slightly distorted by addition of one unit of angular momentum.[45] Angular correlation is somewhat less pronounced in the He $^1D^e$ state. It is, however, still clearly recognizable as a rotor state with two units

of collective angular momentum. The densities plotted in Fig. 6 show that a naive molecular interpretation in terms of collective rotation is, in essence, correct for He ($Z=2$).

We now consider changes in the rotor nature of the states with variation of nuclear charge Z. Figure 6 shows that the appropriately scaled conditional probability densities at the most probable values of r_2 are remarkably similar for He, Li^+, Be^{2+}, and Ne^{8+} in both $^1S^e$ and $^3P^o$ states, and are indeed close to the corresponding densities for DESB wave functions shown in Ref. 12 [cf. Figs. 9(e) and 11(f) of Ref. 12]. This suggests that the $^1S^e$ and $^3P^o$ rotor states of He remain rotorlike for all values of Z, and that an O(4) or DESB description[6,7] of the wave functions is very close to the exact doubly excited function for all Z. For the $^1D^e$ rotor state of He, however, there is a significant change in character as Z is increased. From Fig. 6 we see that the degree of angular correlation in the $^1D^e$ state decreases gradually with increasing nuclear charge until the conditional probability density is almost symmetrical about $\theta_{12}=\pi/2$ for $Z=10$, Ne^{8+}. The latter form of electron distribution is characteristic of the DESB $(K,T=1,0)$ wave function for the $^1D^e$ state (cf. Fig. 12 of Ref. 12) which is just a suitably vector coupled $2p^2$ configuration of hydrogenic orbitals. We therefore conclude that there *is* a *transition* from *collective, rotorlike behavior* in the $^1D^e$, $N=2$ doubly excited state of He to *single-configuration* or *independent-particle-like dynamics* with *increasing nuclear charge*. The dynamics are independent in that correlations apart from those induced by spin symmetry and vector coupling are virtually absent. Put another way, the tendency to mix in higher excited angular configurations and so obtain favorable angular correlation decreases with increasing Z for the $^1D^e$ state, until a single-configuration wave function is obtained at high Z.

It must be stressed that the Sturmian basis used to describe the states of Ne^{8+} (see the Appendix) is sufficiently flexible to represent the amount of angular correlation observed in the rotor states of He. The lack of angular correlation in the $^1D^e$ state of Ne^{8+} therefore reflects an intrinsic property of the wave function rather than an inadequacy of the basis used.

We can infer from these results on the rotor states that a DESB description of intrashell doubly excited states, limited to a basis of product functions of hydrogenic orbitals for the shell of interest, is exact in the limit $Z\rightarrow\infty$. This does not mean that a single configuration provides an adequate description in this limit; the DESB mixings do persist there. This

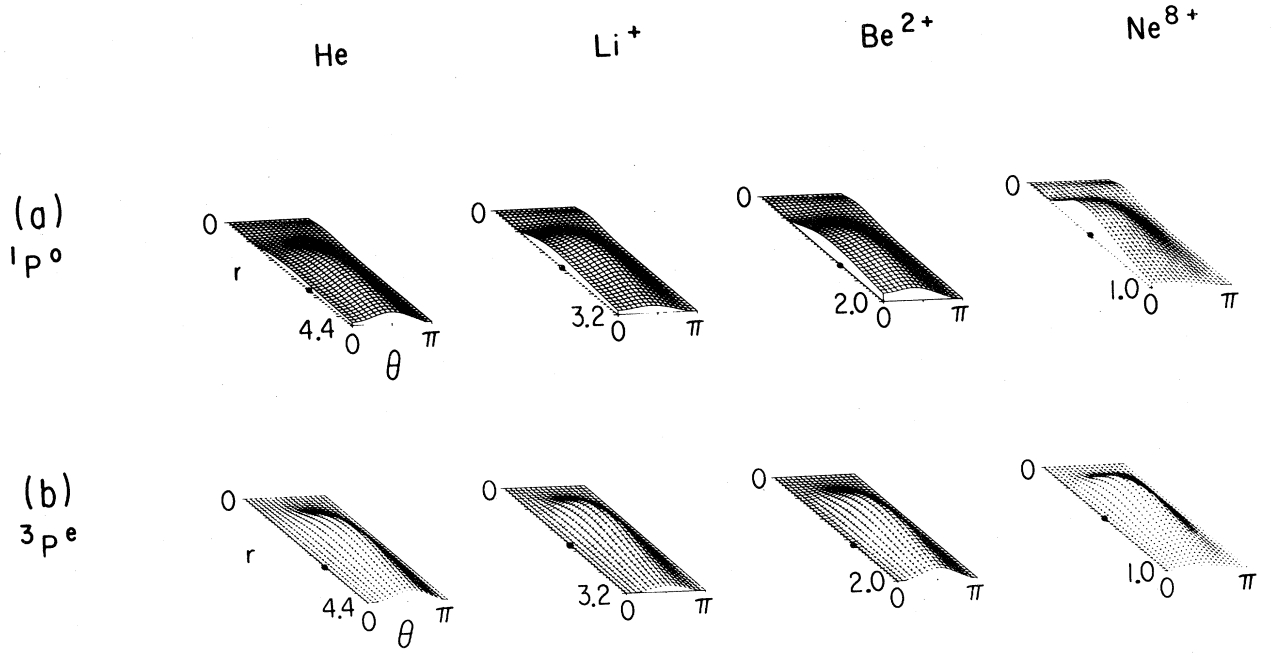

FIG. 7. Conditional probability densities $\rho(r_1,\theta_{12}\,|\,r_2=\alpha)$ for $^3P^e$ and $^1P^o$ states. Nuclear charge $Z=2$ (He), 3 (Li^+), 4 (Be^{2+}), and 10 (Ne^{8+}). Radial coordinates have been scaled to facilitate comparison of wave-function shapes; r_2 has its most probable value in each case.

trend can be understood by examining the Hamiltonian with radial variables scaled by Z^{-1} so that as $Z \rightarrow \infty$ the *intra*shell configuration mixing persists because of the orbital degeneracy, but *inter*shell mixing disappears as Z^{-1}.

We now turn to the densities for the $^1P^0$ and $^3P^e$ states, which are shown in Fig. 7 for He, Li^+, Be^{2+}, and Ne^{8+}, again at the most probable value of r_2 for each state. Consider first the $^1P^o$-$^3P^e$ pair for He. The $^3P^e$ state is constrained by symmetry to have radial nodes at $\theta_{12}=0$ and π, and the conditional probability density rises to a maximum around $\theta_{12}=\pi/2$. In the region $r_1 \sim r_2$ angular correlation shifts the maximum to values of θ_{12} slightly greater than $\pi/2$ so that the cross section of the density at $r_1=r_2\sim 2.9$ bohr is very much like the bending wave function of a rather nonrigid triatomic with 1 quantum of bend (cf. plots in Ref. 33) in qualitative accord with the molecular model. Moreover, the $^1P^o$ density, which is not subject to the same symmetry constraints as the $^3P^e$ state, is very similar to the $^3P^e$ density. Although the $^1P^o$ function must have a node at $r_1=r_2$, $\theta_{12}=\pi$, the actual density is nearly zero for $r_1 \sim r_2$, $\theta_{12}=\pi$ *and* 0. The density associated with the exact wave function is expected to have a Coulomb hole in the region $r_1 \sim r_2$, $\theta_{12} \sim 0$ which will reduce the density there even more. The point is that, for He, densities associated with independent $^3P^e$ and $^1P^o$ functions, which need have no relation to one another in a configurational, independent-particle picture, are in fact remarkably similar. This similarity is very strong evidence for the interpretation of the $^3P^e$-$^1P^o$ pair as near-degenerate partner states having 1 quantum of bending vibration.

As mentioned above, the energy ordering $E(^1P^o) > E(^3P^e)$ is opposite of that found for corresponding l doubled states in linear polyatomics. This reversal of the molecular ordering can be ascribed to the dominance of the greater short-range Coulomb repulsion in the $^1P^o$ state, which is a consequence of the finite electron density at $r_1=r_2$, $\theta_{12}=0$, over the splitting induced by rotation-vibration interactions.

The nodal constraints on the $^3P^e$ function mean that the shape of the two-electron density cannot change drastically with increasing Z, as seen from Fig. 7. In fact, the only major change in the $^3P^e$ density with increasing nuclear charge is a tendency for the distribution to become more symmetric around $\theta_{12}=\pi/2$. Such a symmetric distribution is characteristic of the $2p^2$ $(K,T=0,1)$ DESB state (cf. Fig. 13 of Ref. 12). By contrast, the shape of the $^1P^o$ density changes considerably with Z, passing from an angularly correlated "$v_2=1$ bending" state for He to an "antirotor" state for Ne^{8+} in which there is a maximum in the two-electron density at $r_1=r_2$ and $\theta_{12}=0$ (*not* π) so that the electrons have a strong tendency to sit on top of one another. This antirotor $^1P^o$ density is, in fact, the mirror reflection of the $^3P^o$ density in the $\theta_{12}=\pi/2$ plane and is once again identical with that found using a DESB basis (cf. the caption of Fig. 11, Ref. 12). For high values of the nuclear charge, then, the $^3P^e$ and $^1P^o$ densities are no longer similar, and their molecular interpretation as partner vibrational states breaks down. Once again we have a transformation from a collective correlated state at low Z to a single-configuration independent-particle ("$2s\,2p$") state at high Z.

Figure 8 shows conditional probability densities for the upper $^1S^e$ state of He, Li^+, Be^{2+}, and Ne^{8+} at the most probable values of r_2. The density distribution for He shows marked angular correlation

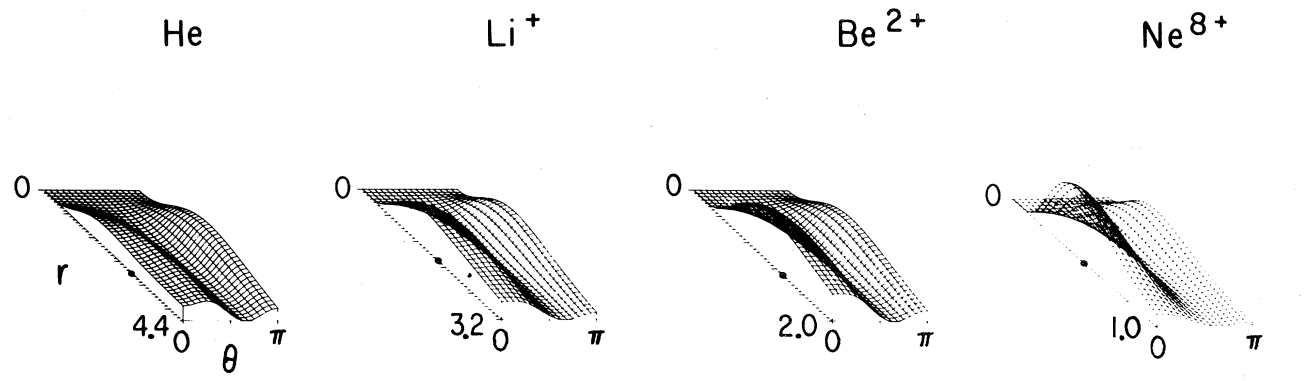

FIG. 8. Conditional probability densities $\rho(r_1,\theta_{12}\,|\,r_2=\alpha)$ for the "$2p^2$" $^1S^e$ state. Nuclear charge $Z=2$ (He), 3 (Li^+), 4 (Be^{2+}), and 10 (Ne^{8+}). Radial coordinates have been scaled to facilitate comparison of wave-function shapes; r_2 has its most probable value in each case.

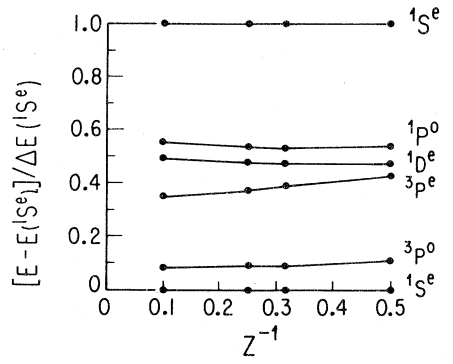

FIG. 9. Calculated $N=2$ intrashell energy levels vs Z^{-1}. Energies are scaled so that the $^1S^e$-$^1S^e$ separation is unity.

and the angular profile at $r_1=r_2$ is in fact qualitatively similar to the $v_2=2$, $l=0$ bending-vibrational wave function for a linear triatomic, having a maximum at $\theta_{12}=0$ and a second maximum at around $\theta_{12}=60°$ [cf. Fig. 3(b) of Ref. 33]. However, as the nuclear charge increases there is a gradual transition to an antirotor state in which electron density is piled up at $\theta_{12}=0$. The shape of the density distribution for Ne^{8+} is identical with that for the $(K,T=-1,0)$ DESB $^1S^e$ wave function for He,[12] which is in turn very similar to the full hydrogenic CI density (Sec. II). We note in passing that the excited $^1S^e$ state of Ne^{8+} with $\theta_{12}\sim 0$ can be considered a kind of "pairing state" or eigenfunction of a δ-function interaction,[19,35] and presumably has a high interelectronic repulsion energy. Such antirotor states should be contrasted, rather than identified, with so-called Wannier states, which have the most probable region of $\theta_{12}\sim\pi$ and large autoionization widths (cf. Ref. 46).

To conclude this section we show in Fig. 9 doubly excited $N=2$ intrashell energies versus Z^{-1} scaled so that the upper $^1S^e$ state has unit energy with respect to the lower $^1S^e$ state. The notable feature of this plot is that, despite the relatively large qualitative changes we have seen in the wave functions for some states as Z is varied, the scaled pattern of energy levels changes relatively little. As Z is increased, the $^1P^o$ and $^3P^e$ levels move slightly further apart, while the ratio

$$[E(^1D^e)-E(^3P^o)]/[E(^3P^o)-E(^1S^e)]$$

departs more and more from the rigid-rotor value 2:1, but there are no crossings of levels. This brings out the point that, despite the fact that an empirical analysis of energy-level patterns suggested the molecular interpretation of doubly excited states in the first place, the qualitative form of the level pattern is not necessarily a conclusive indicator of the constants of the motion or of the shape of the wave functions as Fig. 9 shows.

IV. INTERSHELL DOUBLY EXCITED STATES: He

In this section we examine probability densities for the lowest S^e and P^o states (both singlet and triplet) of the $n_1=2$, $n_2=3$ *intershell* doubly excited manifold of He, with a view to possible extension of the molecular model to intershell states. The graphs we present give the first detailed representation of the nature of electron correlation in intershell states and are therefore of considerable intrinsic interest.

Energy levels and eigenfunctions for the intershell doubly excited states are calculated using the same Sturmian basis as for the intrashell He states (cf. Sec. II and the Appendix). This basis is particularly well suited to describe long-range angular correlation in the region $r_1\sim r_2$ and it is possible that the extensive radial correlation likely to occur in intershell states may not be as well represented with Sturmians. It may even be that, for the intershell states, hydrogenic CI functions provide a more accurate representation of the true wave function than do Sturmians. Table III compares eigenvalues for hydrogenic CI functions[23] with those obtained from stabilized Sturmian CI calculations for the four states of interest. For the $^1P^o$ state, it is necessary to change the exponents in the intrashell Sturmian basis to obtain agreement with the (lower-energy) hydrogenic result; for the other states, agreement with the hydrogenic results is quite reasonable using the intrashell basis. Bearing in mind these reservations concerning the use of a Sturmian basis, we present results here only for the lowest S and P states of the intershell manifold. A more extensive study using a hydrogenic CI basis is reserved for later communications.

Figure 10 shows single-particle radial distribution functions calculated for the following states of He: "$2s\,3s$" $^1S^e$, "$2s\,3s$" $^3S^e$, "$2s\,3p/2p\,3s$" $^3P^o$, "$2s\,3p/2p\,3s$" $^1P^o$. The peak corresponding to the $N=2$ shell is clearly visible at $r\sim 2.5$–3.0 bohr, as is

TABLE III. Energy levels for $n_1=2$ and $n_2=3$ intershell doubly excited states of He: $-E$ (Ry).

	Sturmian CI	Hydrogenic CI
$^1S^e$("$2s\,3s$")	1.173 61	1.176 28
$^3S^e$("$2s\,3s$")	1.201 84	1.204 20
$^1P^o$("$2s\,3p/2p\,3s$")	1.194 00[a]	1.193 13
$^3P^o$("$2s\,3p/2p\,3s$")	1.163 63	1.166 71

[a]Different exponents in Sturmian basis.

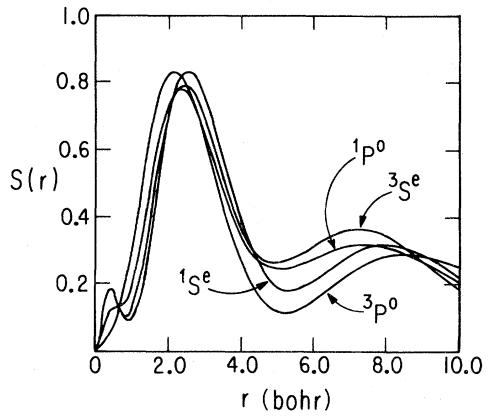

FIG. 10. Single-particle radial density distribution function $r^2S(r)$ for $n_1=2$ and $n_2=3$ He intershell states: $^1S^e$, $^3S^e$, $^1P^o$, and $^3P^o$.

the $N=3$ peak at $r\sim 7.5$—8.0 bohr.

The molecular model for intrashell doubly excited states can be extended to intershell states by associating radial excitation of one electron to a higher shell with *stretching vibrations* of the "bonds" in the XY_2 molecule (Fig. 1). In this very simple scheme, the lowest $^1S^e$ and $^3S^e$ states of the $n_1=2$, $n_2=3$ intershell manifold correspond to the first excited states of the symmetric and antisymmetric stretching modes, respectively. The lowest $^3P^o$ and $^1P^o$ states are then the associated respective rotor states based on the vibrationally excited S states.

Figure 11 displays probability densities for the $^1S^e$, $^3P^o$, $^3S^e$, and $^1P^o$ intershell states of He at four values of r_2: $r_2=0.1$, 2.5, 5.0, and 7.5 bohr. The most probable configurations are those for which r_2 corresponds to a shell radius, i.e., $r_2=2.5$ or 7.5 bohr.

It is immediately clear from Fig. 11 that, while all states show considerable angular correlation, the one-particle shell structure determines the pattern of *radial* correlation. Comparison of the plots for the $^1S^e$ and $^3S^e$ states reveals the role of the exclusion principle in shaping the wave function. For example, when $r_2=2.5$ bohr, there is an appreciable probability of finding both electrons at the same distance from the nucleus ("in the same shell") for the $^1S^e$ state, while for the $^3S^e$ state the Pauli principle

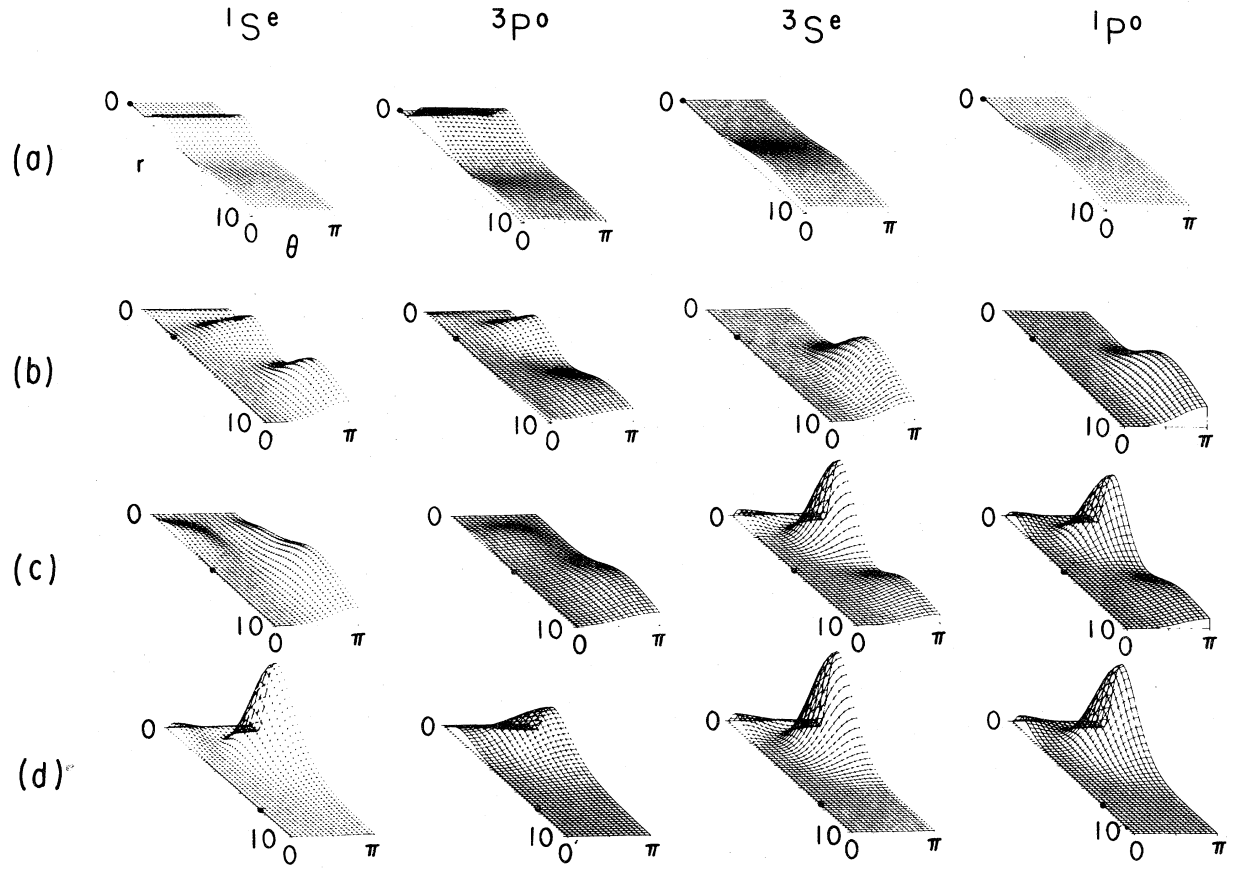

FIG. 11. Conditional probability densities $\rho(r_1,\theta_{12}\,|\,r_2=\alpha)$ for He $n_1=2$, $n_2=3$ intershell states: $^1S^e$, $^3S^e$, $^1P^o$, and $^3P^o$. (a) $\alpha=0.1$ bohr; (b) $\alpha=2.5$ bohr; (c) $\alpha=5.0$ bohr, (d) $\alpha=7.5$ bohr.

forces the other electron out to a distance of ~ 7.5 bohr ("into a different shell"). When $r_2 = 7.5$ bohr, both densities look very much the same, from which we can infer that there is little admixture of the "$3s^2$" configuration into the $^1S^e$ state. The $^3S^e$ state is constrained to have a node at $r_1 = r_2$ for all values of θ_{12}, so that the resulting electron density inevitably resembles that for an antisymmetric-stretch type of radial excitation. There is no such constraint on the $^1S^e$ state.

Comparison of the S-state densities with those for the corresponding P states shows the extent to which collective rotation occurs in the intrashell states. While the plots of Fig. 11 indicate that there is a significant amount of angular correlation in both the $^1S^e$ and $^3P^o$ states, the $^3P^o$ density corresponds only very approximately to collective rotation of the $^1S^e$ electron distribution. On the other hand, the $^3S^e$ and $^1P^o$ densities are very similar for all values of r_2 so that in this case it appears that the $^1P^o$ state does represent a genuine rotor state based upon the "antisymmetric stretch" ($^3S^e$). In this connection it is very interesting to note that extension of the supermultiplet classification scheme to intershell states[47] has shown that the rotor-vibrator pattern is much better defined for states corresponding to collective excitations based on the "antisymmetric stretch" ($^3S^e$) than those based on the "symmetric stretch" ($^1S^e$). The full elucidation of these findings will require further systematic studies of the two-electron densities associated with intershell states.

V. CONCLUSIONS

In the present work we have examined plots of conditional probability densities for doubly excited states of two-electron atoms calculated from Sturmian CI wave functions in order to determine the extent to which a naive molecular picture of electron correlation is valid. Our plots for He ($Z = 2$) reveal a remarkable degree of collective rotor-vibrator behavior in the $N = 2$ shell, showing that the molecular interpretation of the doubly excited spectrum due to Kellman and Herrick[17] is a useful qualitative picture of the dynamics. We have deliberately avoided any discussion of the interpretation of associated molecular constants, such as the moment of inertia or bending-vibration frequency, since a quantitative treatment is not necessarily useful at this stage. It should only be noted that moments of inertia derived from fits of doubly excited spectra to molecular term formulas are anomalously large compared with rigid-rotor values calculated for two electrons at ~ 2.8 bohr from the nucleus; the interpretation of this result remains problematic.

Upon increasing the nuclear charge some states ($^1D^e, ^1P^o$) are seen to show a steady transition from a correlated, collective type of wave function to a single-configuration or independent particle wave function in which there is very little mixing in of excited high angular momentum states, while others (the rotor states "$2s^2$" $^1S^e$ and $^3P^o$) remain essentially unchanged. The upper "$2p^2$" $^1S^e$ state evolves from an angularly correlated bending state to an antirotor pairing state in which the electrons have a strong tendency to remain on the same side of the nucleus. The $^3P^e$ state provides an example where symmetry constraints determine the shape of the wave function to a large degree. Our results enable us to infer the exactness of the DESB description of doubly excited states in the limit $Z \to \infty$.

In the more general context of the nature of quantum states in few-body systems, the above findings should be compared with our previous studies of model problems such as particles on spheres (either the same[33] or concentric[34]). For example, in the case of particles on concentric spheres (POCS), we have observed a smooth transition from collective to independent-particle wave functions as the radius-ratio of the two spheres is increased for both Coulomb and repulsive Gaussian interparticle interactions.[34] Similarly, there is a transition to independent-particle behavior with increasing energy for two particles on the same sphere interacting through a repulsive Gaussian potential.[33]

Finally, the discovery that few-electron atoms may under some conditions exhibit collective moleculelike behavior suggests the possibility of finding independent-particle motions of nuclei in highly excited vibrational states of small polyatomic molecules. One conceivable way to induce such behavior would involve progressive excitation of a local-mode[48] (bond) vibration in, for example, H_2O, to the point where there is hindered rotation of an OH "core" in the field of the outer proton. In this case the individual proton angular momenta begin to become more nearly good constants of the motion. Preliminary model calculations using the Murrell-Sorbie[49] potential surface for H_2O indicate that this type of intramolecular motion may occur after 7 or

TABLE IV. Exponents defining the Slater orbital basis used for calculation of doubly excited CI wave functions.

	Single-particle angular momentum l					
Nuclear charge Z	0	1	2	3	4	5
2	0.7	1.0	1.0	1.0	1.0	1.0
3	1.2	1.5	1.5	1.5	1.5	1.5
4	1.6	2.0	2.0	2.0	2.0	2.0
10	4.0	5.0	5.0	5.0	5.0	5.0

TABLE V. Number of function of each symmetry type in the Sturmian CI basis.

	$^1S^e$	$^3P^o$	$^1D^e$	$^1P^o$	$^3P^e$
Number	63	75	89	75	35

8 quanta have been pumped into a single O—H bond. Further investigation of these intriguing commonalities of atoms and molecules[29,30] continues.

ACKNOWLEDGMENTS

We are very grateful to Professor J. Callaway for providing us with a listing of his two-electron program. G.S.E. would like to thank the United Kingdom Science Research Council for the award of a North Atlantic Treaty Organization fellowship. This work was supported in part by a grant from the National Science Foundation.

APPENDIX

As discussed in Section II, the CI calculations reported here use a Sturmian radial basis constructed from Slater orbitals of the form (5). The basis we use contains single-particle angular momenta up to $l_{\max}=5$ with the following maximum orbital principal quantum numbers n: $l=0$, $n=7$; $l=1$, $n=6$; $l=2$, $n=6$; $l=3$, $n=6$; $l=4$, $n=6$; $l=5$, $n=6$. All Slater functions with the same l value have the same exponent ξ. Table IV gives values of the exponents used for each nuclear charge Z, while Table V shows the number of functions of each symmetry type.

*Present address: Department of Chemistry, Cornell University, Ithaca, New York 14853.

[1]J. W. Cooper, U. Fano, and F. Prats, Phys. Rev. Lett. 10, 518 (1963).
[2]C. E. Wulfman, Phys. Lett. 26A, 397 (1968).
[3]J. S. Alper and O. Sinanoglu, Phys. Rev. 177, 77 (1969).
[4]J. S. Alper, Phys. Rev. 177, 86 (1969).
[5]J. Macek, J. Phys. B 1, 831 (1968).
[6]C. E. Wulfman, Chem. Phys. Lett. 23, 370 (1973).
[7]O. Sinanoglu and D. R. Herrick, J. Chem. Phys. 62, 886 (1975).
[8]C. D. Lin, Phys. Rev. A 10, 1986 (1974).
[9]U. Fano, Phys. Today 29, (9), 32 (1976).
[10]S. I. Nikitin and V. N. Ostrovsky, J. Phys. B 9, 3141 (1976).
[11]S. I. Nikitin and V. N. Ostrovsky, J. Phys. B 11, 1681 (1978).
[12]P. Rehmus, M. E. Kellman, and R. S. Berry, Chem. Phys. 31, 239 (1978).
[13]P. Rehmus and R. S. Berry, Chem. Phys. 38, 247 (1979).
[14]M. E. Kellman and D. R. Herrick, J. Phys. B 11, L755 (1978).
[15]D. R. Herrick and M. E. Kellman, Phys. Rev. A 21, 418 (1980).
[16]D. R. Herrick, M. E. Kellman, and R. D. Poliak, Phys. Rev. A 22, 1517 (1980).
[17]M. E. Kellman and D. R. Herrick, Phys. Rev. A 22, 1536 (1980).
[18]H.-J. Yuh, G. S. Ezra, P. Rehmus, and R. S. Berry, Phys. Rev. Lett. 47, 497 (1981).
[19]F. Iachello and A. R. P. Rau, Phys. Rev. Lett. 47, 501 (1981).
[20]C. D. Lin, Phys. Rev. A 25, 76 (1982).
[21]C. D. Lin, Phys. Rev. A 25, 1535 (1982).
[22]M. Crance and L. Armstrong, Jr., Phys. Rev. A 26, 694 (1982).
[23]L. Lipsky, R. Anania, and M. J. Conneely, At. Data Nucl. Data Tables 20, 127 (1977).
[24]J. Callaway, Phys. Lett. A 66, 201 (1978).
[25]M. Moshinsky, Phys. Rev. 126, 1880 (1962).
[26]M. J. Englefield, *Group Theory and the Coulomb Problem* (Wiley, New York, 1972).
[27]D. R. Herrick, Adv. Chem. Phys. 52, 1 (1982).
[28]G. Herzberg, *Molecular Spectra and Structure* (Van Nostrand, New York, 1945), Vol. II.
[29]R. S. Berry, in *Proceedings of the Sixteenth Jerusalem Symposium on Quantum Chemistry and Quantum Molecular Biology,* edited by J. Jortner and B. Pullman (Reidel, Dortrecht, Holland, 1982).
[30]R. S. Berry, G. S. Ezra, and G. A. Natanson, in *Proceedings of 4th International Congress in Quantum Chemistry* (Reidel, Dortrecht, Holland, 1982).
[31]P. Rehmus, C. C. J. Roothaan, and R. S. Berry, Chem. Phys. Lett. 58, 321 (1978).
[32]H.-J. Yuh and R. S. Berry (unpublished).
[33]G. S. Ezra and R. S. Berry, Phys. Rev. A 25, 1513 (1982).
[34]G. S. Ezra and R. S. Berry (unpublished).
[35]D. R. Herrick, Phys. Rev. A 22, 1346 (1980).
[36]R. B. Walker and R. E. Wyatt, J. Chem. Phys. 57, 2728 (1972); S. H. Harms and R. E. Wyatt, *ibid.* 62, 3162, 3173 (1975); A. B. Elkowitz and R. E. Wyatt, *ibid.* 62, 3683 (1975); *ibid.* 63, 702 (1975); S. H. Harms, A. B. Elkowitz, and R. E. Wyatt, Mol. Phys. 31, 177 (1976).
[37]A. K. Bhatia and A. Temkin, Rev. Mod. Phys. 36, 1050 (1964); A. K. Bhatia, A. Temkin, and J. F. Perkins, Phys. Rev. 153, 177 (1967); A. K. Bhatia and A. Temkin *ibid.* 182, 15 (1969); A. K. Bhatia, P. G. Burke, and A. Temkin, Phys. Rev. A 8, 21 (1973); 10, 459(E) (1974); A. K. Bhatia and A. Temkin, *ibid.* 8, 2184 (1973); 10, 458(E) (1974); A. K. Bhatia, *ibid.* 6, 120

(1972); A. K. Bhatia and A. Temkin, *ibid.* 11, 2018 (1975); A. K. Bhatia, *ibid.* 15, 1315 (1977).

[38]J. C. Slater, *Quantum Theory of Atomic Structure* (McGraw-Hill, New York, 1960), Vol. II.

[39]E. A. Hylleraas, Z. Phys. 38, 739 (1933).

[40]E. Holøien, Proc. Phys. Soc. London, Sect. A 71, 357 (1958); 72, 141 (1958).

[41]H. Shull and P.-O. Löwdin, J. Chem. Phys. 30, 617 (1959).

[42]B. G. Adams, J. Cizek, and J. Paldus, Int. J. Quantum Chem. XXI, 153 (1982).

[43]B. T. Smith, J. M. Boyle, J. J. Dongarra, B. S. Garbow, Y. Ikebe, V. C. Klema, and C. B. Moler, in *Lecture Notes in Computer Science,* edited by G. Goos and J. Hartmanis (Springer, New York, 1976), Vol. 6; B. S. Garbow, J. M. Boyle, J. J. Dongarra, and C. B. Moler, *ibid.* Vol. 51.

[44]L. Lipsky and A. Russek, Phys. Rev. 141, 59 (1966).

[45]H. Herold and H. Ruder, J. Phys. G 5, 341 (1979); G. Wunner, H. Ruder, and M. Reinecke, *ibid.* 6, 1359 (1980).

[46]P. Rehmus and R. S. Berry, Phys. Rev. A 23, 416 (1981).

[47]M. E. Kellman and D. R. Herrick (unpublished).

[48]For a recent review see B. R. Henry, Vib. Spectra Struct. 10, 269 (1981).

[49]K. S. Sorbie and J. N. Murrell, Mol. Phys. 29, 1387 (1978).